



Research Article

Development of a remote shape memory alloy experiment for engineering education

Ning Wang^{1*}, Jun Weng², Xuemin Chen³, Gangbing Song², Hamid Parsaei⁴

¹Department of Electrical and Computer Engineering, University of Houston, Houston TX, USA

²Department of Mechanical Engineering, University of Houston, Houston TX, USA

³Department of Engineering Technology, Texas Southern University, Houston TX 77004, USA

⁴Department of Mechanical Engineering, Texas A&M University at Qatar, Doha, Qatar

*nwang@uh.edu

Abstract

In this paper, we present and compare two different implementation approaches for a remote shape memory alloy (SMA) experiment development. The remote SMA experiment aims to offer students a hands-on experience in testing and control of an SMA wire actuator via remote laboratory platform. One approach is based on the LabVIEW remote panel and other one is based on a novel unified remote laboratory framework. The new remote SMA experiment based on a novel unified framework is implemented at Texas A&M University at Qatar (TAMUQ) for mechanical engineering teaching. With this new remote experiment, the user can remotely conduct the SMA experiment by using any portable device without installing any plug-in.

Introduction

In the last two decades, the engineering education community has carried out numerous initiatives to develop and implement a remote laboratory for engineering education. This trend arose from the availability of innovative software packages for instrumentation and simulation, as well as the necessity to better support active and collaborative learning. In the early remote laboratory system, most solutions for remote experimentation relied on client-server architecture (Gillet et al, 1997). From the point of view of client-server

Cite this article as: Wang N, Weng J, Chen X, Song G, Parsaei H. Development of a remote shape memory alloy experiment for engineering education, *Engineering Education Letters* 2015;2 <http://dx.doi.org/10.5339/eel.2015.2.pp1-20>

software architecture, remote laboratory architects have no choice but to build a middleware, allowing remote clients to connect to the local computer that handles the device (Gravier et al, 2008). In many client-server architecture software solutions, National Instrument's LabVIEW (Laboratory Virtual Instrument Engineering Workbench) is one of the most popularly deployed technologies for remote panel interfaces over the internet (Duro et al, 2008). Despite its great advantages in effectiveness and rapid prototyping, LabVIEW has been plagued by software issues from its runtime engine. Furthermore, any updates to the LabVIEW front panel can result in version errors on the client side due to the non-compatibility of the runtime engines. The traditional remote Shape Memory Alloy (SMA) experiment was developed based on the LabVIEW remote panel. It can be conducted remotely with LabVIEW remote panel plug-in.

With the development of computer technology, browser-server architecture is becoming increasingly more stable, and new technologies have since been developed to support more complex internet applications based on a web browser. The user remotely accesses and controls the instrument via a user interface in a web browser. To adopt the browser-server architecture for the remote laboratory, LabVIEW integrated a new feature to interact with the virtual instruments (VIs) by using REpresentational State Transfer (RESTful) web services technology. However, there are still some challenges in this software system deployment and the limitation of network security management in the colleges. In order to solve the challenge of system deployment, we proposed and developed a novel unified remote laboratory framework which allows distributed online experiments to work in any internet browser, independent of any additional plug-ins, and also resolved some challenging issues of developing cross-browser and cross-device web user interfaces (Wang et al, 2014). This novel unified framework is designed using browser-server architecture, and developed based on the Web 2.0 technology. We have used this framework to implement some remote control engineering experiments successfully. For example, the new SMA remote experiment with the novel unified framework was built up at Texas A&M University at Qatar (TAMUQ).

In this paper, we present and compare two different implementation approaches for the remote SMA experiment integration and implementation. We list the difference of these two solutions, and give the advantage of the new solution based on the novel unified framework. The users can conduct this new remote SMA experiment with web browsers without any plug-in. This new solution represents a prodigious improvement on the remote SMA experiment development.

Control of the shape memory alloy

Shape memory alloy (SMA) has two phases, martensite and austenite. By increasing the temperature, SMA will change from martensite to austenite. An SMA wire is easily lengthened in the martensite phase at the lower temperature and its length will return back to the original length in the austenite phase at higher temperatures. It is known as the Shape Memory Effect (SME). The force generated by SMA wire in the austenite phase is large and the SME is controllable.

SMA has a nonlinear response because of the hysteresis of SME. A model of SMA is hard to build (Song and Ma, 2007, Majima et al, 1999, Fan and Song 2005, Song and Quinn 2004). In the theory of nonlinear control, there are several methods we can use, for instance by using multiple accurate linear equations together to simulate the Fuzzy PID controller (Kilicarslan et al, 2008, Sehab 2007), Bang-Bang and saturation compensator (Cai and Abdalla 1993), the nonlinear model (Lentijo 2004), and sliding mode-based robust controller (Bang 2005, Cepeda-Gomez 2010, Tai and Ahn 2010, Kizmaz 2010, Lowe and Zohdy 2010).

In a nonlinear system, the uncertainties of the system are unpredictable or hard to predict in linear equations. The uncertainty in the control of SMA is the hysteresis when SMA returns to its original length. Like many nonlinear system controls, we design nonlinear compensators to control the length change of SMA according to the feedback of the length change of SMA. We will review three conventional robust controllers and compensators used in nonlinear control, bang-bang compensator, the saturation compensator, and the smooth compensator. In the comparison, we will see the smooth compensator provides more accurate feedback control over the other two compensators (Song and Mukherjee 1998, Cai and Song 1993). That is also the reason why we use the smooth compensator in the control of SMA in our SMA experiment.

Consider the tracking control of SMA and we use the equation from Dr. Gangbing Song's successful implementation of nonlinear robust control on SMA. It uses a smooth compensator to control the displacement of SMA wire. The input is electrical current and the output is the length change of SMA wire. Equations (1) to (3) are the mathematical model of the compensator,

$$e = y - y^d, \quad (1)$$

$$r = \dot{e} + \beta e, \quad (2)$$

$$u = u_f - Kr - \rho \tanh(ar). \quad (3)$$

The aim of the control system is to control the displacement of SMA length.

- y is the feedback of the system - which is the real position of the SMA.
- y^d is the desired position defined by the users.
- e is the error between the real position and the desired position.
- \dot{e} is the derivative of the position error.
- u_f is a feedforward term to compensate the heat losses and provide a voltage to heat up the SMA.
- K and r expressed in Equation (3) are proportional plus derivative (PD) term.
- $\rho \tanh(ar)$ is the smooth robust compensator.

The PD term in the feedback control increases the damping to reach the stable state of the system. The smooth robust compensator compensates the hysteresis of SMA, uncertainties in the system and disturbances from the environment. u is the electrical current or the voltage applied to SMA to control the length change of it. β , ρ , and a are constants tuned in the experiment.

The feedback controller with the bang-bang compensator has expressions shown in Equation (4), where the feed forward term and the PD term are the same as that in smooth compensator; and the difference is the bang-bang robust compensator, $\rho \text{sign}(r)$ defined by Equation (5),

$$u = u_f - Kr - \rho \text{sign}(r) \quad (4)$$

$$\text{sign}(r) \triangleq \begin{cases} 1, & \text{if } r > 0 \\ -1, & \text{if } r < 0 \end{cases} \quad (5)$$

In the bang-bang compensator, when r is larger than zero, the gain of $\text{sign}(r)$ is positive one; when r is less than zero, the gain of $\text{sign}(r)$ is negative one. The r term defined in Equation (2) is dependent on the position error and the derivative of the position error.

The feedback controller with the saturation compensator has expression shown in Equation (6), where the difference comparing to Equation (5) is the saturation term, $\rho \text{sat}\left(\frac{r}{\varphi}\right)$, defined by Equation (7),

$$u = u_f - Kr - \rho \text{sat}\left(\frac{r}{\varphi}\right) \tag{6}$$

$$\text{sat}\left(\frac{r}{\varphi}\right) \triangleq \begin{cases} 1, & \text{if } r > \varphi \\ -1, & \text{if } r < -\varphi \\ \frac{r}{\varphi}, & \text{if } |r| < \varphi \end{cases} \tag{7}$$

In the saturation compensator, r is defined by Equation (2), and φ is constant defined by the user. The saturation compensator has a mathematical expression shown in Equation (7): when the variable r is larger than the defined constant φ , the gain of the saturation is positive one; when the variable r is less than the negative constant φ , the gain of the saturation is negative one; and when the absolute value of the variable r is less than the constant φ , the saturation equals to the value of r divided by the constant φ , which is $\frac{r}{\varphi}$.

Figure 1 shows the chattering results of imperfect control switch and Figure 2 shows the three compensators. The bang-bang compensator has an instant change in the magnitude from negative one to positive one; however, the saturation compensator has a linear increase in the magnitude change from negative one to positive one. The smooth compensator has more accurate results comparing to the bang-bang compensator and saturation compensator. The smooth compensator follows the function, $\tanh(ar)$, in the change from negative one to positive one. We can design and tune the value of a in Equation (3) and the value of β in Equation (2) to affect the shape of the smooth compensator shown in Figure 2 (c) till we find a controller with good performance.

In the comparison of three compensators in Figure 2, the smooth compensator in Figure 2 (c) provides more accurate control. Thus, we use the smooth compensator in our SMA actuator in SMA device.

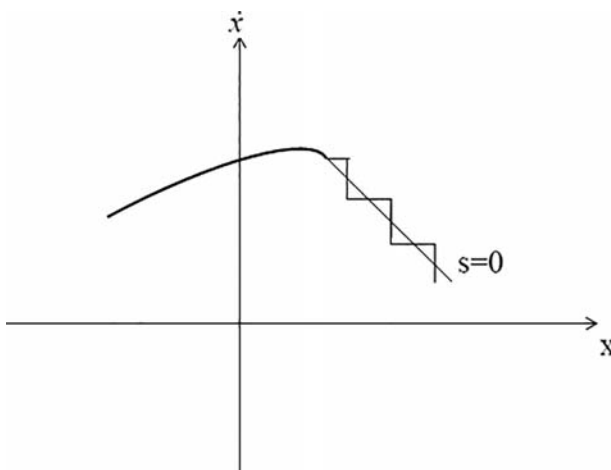


Figure 1: Chattering as a result of imperfect control switching.

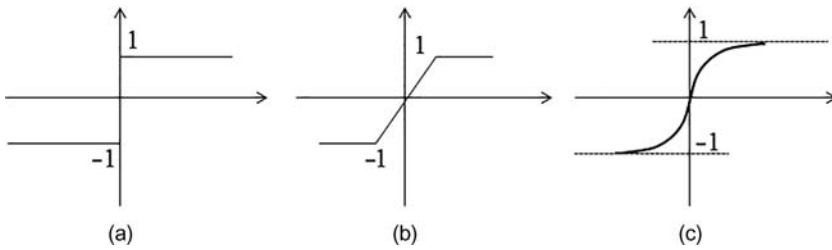


Figure 2: Comparison of three compensators: (a) the bang-bang compensator, (b) the saturation compensator, and (c) the smooth compensator.

Remote SMA experiment

The SMA experiment is developed to demonstrate and analyze the characteristics of shape memory alloys. It is used to study the hysteresis behavior of the wire actuator (SMA) and how the driving frequency changes the hysteresis loop. The experiment can apply sinusoidal driving signals (AC) of 16.4 V in magnitude and respectively from 1/30Hz to 1/50Hz in frequency to the SMA actuator. Students can observe the wire movement through the webcam in the remote laboratory. They can record a number of cycles for each test. Saved data are applied voltage, the displacement of the wire actuator, and the time in seconds. The data will be used for future analysis.

The experiment consists of an SMA wire connected to the electronic circuitry that controls the voltage going to SMA wire. A displacement sensor is also attached to the SMA wire to sense the motion caused by the SMA during heating and cooling through the applied electric voltage. This experiment uses real instrumentation and components at a different location than where they are being controlled by the user and consists of two parts; SMA experiment software development and SMA experiment hardware equipment setup. For the traditional remote SMA experiment with LabVIEW, we used LabVIEW to develop the software part which includes user interface which was called the LabVIEW Remote Panel and experiment control application. However, for the new remote SMA experiment, we used the novel unified framework to implement the software part. The advantage of the novel unified framework is that it is plug-in free and runs in different web browsers.

Hardware setup for remote SMA experiment

The SMA device, as shown in [Figure 3](#) and [Figure 4](#), is assembled by using both fabricated and off-the-shelf components. The main frame uses an L-shaped aluminum bar fixed by screws. There are plexi-glass sheets fixed on several sides of the SMA to protect and decorate the experiment. On the bottom, blue LED lights are used to light up the experiment. In the middle of the SMA device, a red block is lifted by SMA wire and pulled down by two springs. The experiment consists of a workstation, NI DAQ 6008 USB (data acquisition), and a DC power supply, a SSR (solid state relay), a webcam, and SMA wires. A PC workstation runs LabVIEW to control the voltage applied on the SMA wire. NI DAQ 6008 USB is a hardware device talking to the experiment and the PC. It generates voltage output based on the signal from LabVIEW and senses voltage changes in the experiment to control the amount of voltage to SMA wire.

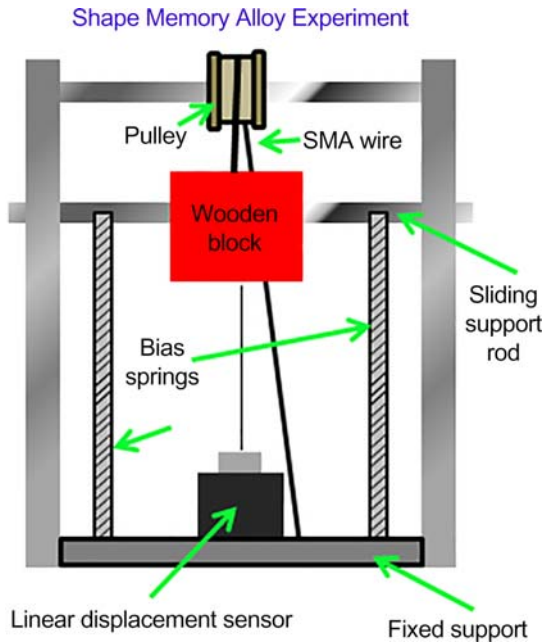


Figure 3: Schematic diagram of SMA device.

The DC power supply is used to generate a consistent voltage on SMA. PWM (pulse-width modulation) is used to control the voltage by using a SSR. The SSR can switch on and off swiftly to have a voltage value defined by the user even using a DC power supply. The camera is used to view the experiment change remotely. By applying voltage on SMA wire, the temperature of SMA will increase and the length of the wire will decrease.

Control of the SMA experiment

In the experiment, two parameters need to be controlled; one is the displacement of the block and the other one is the desired value of voltage applied on SMA wire. The voltage applied on the SMA is controlled using PWM and the displacement of the block can be controlled using a sliding mode based controller. PWM has benefits of generating signals with ease to change its frequency, voltage magnitudes and forms (Vasca and Lannelli 2012). It compares with a carrier signals and the desired signals to switch the circuitry connected with the DC power supply in series on and off to achieve the same effects as the desired signals in an efficient and flexible way. In the displacement control of SMA, the response of SMA is nonlinear due to hysteresis. Based on the successful research done before, a sliding mode-based controller is very competitive with other nonlinear controllers, like bang-bang control for our purpose (Grant and Hayward 1997). The algorithm of PWM and a sliding mode-based controller are programmed and implemented in LabVIEW VI. The data of the real displacement of SMA is collected by NI DAQ 6008. The programmed VI reads the real displacement and then the controller module in VI computes desired voltages before the PWM module in VI. Controlled signals are then output

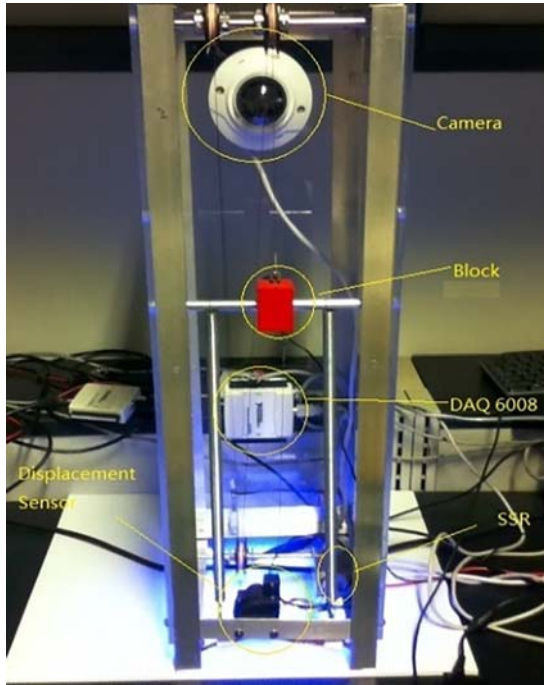


Figure 4: SMA experiment.

from the VI through DAQ 6008 to the connected circuitry to achieve the displacement control of SMA.

A sliding mode-based controller for displacement control

Since the system was nonlinear due to the hysteresis of SMA, a sliding mode-based controller was designed based on the successful controller of an SMA wire actuated flap. Based on [Equation \(1\) to \(3\)](#), the controller is shown in the following,

$$V = V_f - Kr - \rho \tanh(ar). \quad (8)$$

After tuning in the experiment, [Eqn. \(2\)](#) and [Eqn. \(8\)](#) become,

$$r = \dot{e} + 15e \quad (9)$$

$$V = 10 - 15r - 1 \tanh(-1r), \quad (10)$$

Where V is the output voltage.

Pulse width modulation

PWM has the benefit of generating signals with ease to change its frequency, voltage magnitudes and forms to control the output applied on the experiment ([Bowes and Grewal 1998](#), [Boost and Ziogas 1988](#), [Black 1953](#)). By comparing a carrier signal, $c(t)$, to a reference signal, $r(t)$ as shown in

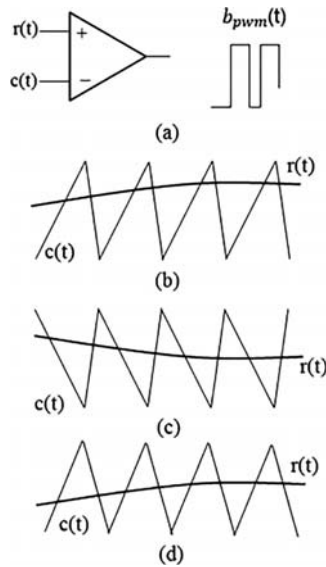


Figure 5: Constant frequency PWM implemented by a comparator with different carrier signals.

Figure 5, it generates a constant-frequency (CF) PWM signal. In CF PWM, there are three types of carrier signals commonly used, saw-tooth carrier (Figure 5b), inverted saw-tooth carrier (Figure 5c), and triangle carrier (Figure 5d). In our experiment, we will use CF PWM because we are using signals of constant frequency for the voltage output applied on the SMA actuator.

The reference signals have a leading edge and a trailing edge. In the saw-tooth carrier, the leading edge is rising instantly and the trailing edge (falling) is modulated as the reference signal level changes, which is referred to as constant-frequency trailing-edge modulation.

In inverted saw-tooth carrier, the trailing is falling instantly and the leading edge (rising) is modulated as the reference signal level changes, which is referred to as constant-frequency leading-edge modulation.

In triangle carrier, the leading edge and the trailing edge are both modulated. Two edges are symmetric to ensure the pulse is placed in the middle of a carrier cycle when the reference signal is a constant. It is referred to as constant-frequency double-edge modulation.

Trailing-edge modulation is used most in DC-DC conversions, and double-edge modulation is commonly used in AD-DC and DC-AC conversions, because double-edge modulation can reduce the effects from some harmonics in sinusoidal signals.

There are two sets of PWM signals generated separately with either of the reference signals of trailing-edge modulation and double-edge modulation, as depicted in Figure 6 and Figure 7. As we can see from two figures, the reference signals, $r(t)$, is comparing with the carrier signal, $c(t)$. When the amplitude of the reference signal is larger than the amplitude of the carrier signal at time t , the PWM signal, b_{pwm} , has a step value at the same time instant. Similarly, when the amplitude of the reference signal is smaller than the carrier signal, the PWM signal has a value of zero.

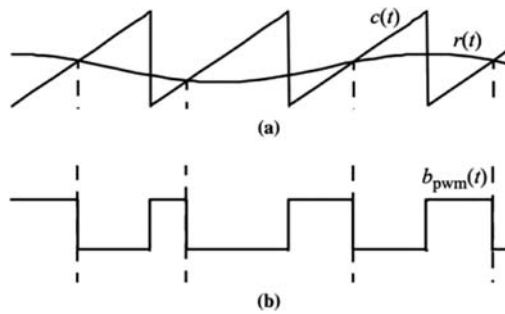


Figure 6: Trailing-edge modulation.

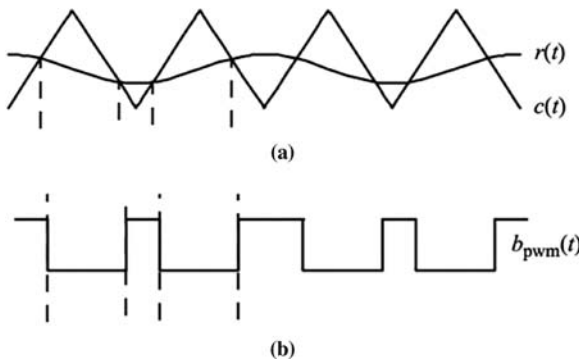


Figure 7: Double-edge modulation.

In the experiment, we used double-edge modulation instead of trailing-edge modulation. The carrier signal in the SMA experiment is a sinusoidal wave with frequencies from 1/30Hz to 1/50Hz. The frequency of the carrier signal is adjustable by the client. The parameters of the reference signal of SMA experiment are tuned in the real experiment to ensure the best outcome of the performance.

Software development for remote SMA experiment

The software development for remote SMA experiment includes two parts, user interface development and server control application development. In this section, we present two different implementation approaches for the remote SMA experiment development.

Remote SMA experiment based on LabVIEW Remote Panel

Several versions of LabVIEW have furthered the ability to develop distributed applications: TCP/IP, Internet Toolkit, VI Server, Front Panel Web Publishing, Remote Data Acquisition (RDA), DataSocket, and so on. In addition, several third party toolkits have enabled internet-based VI control: LabVNC and AppletVIEW. Then, of course, there has always been PC Anywhere and other similar applications that provide general remote control of a PC. With enough effort, you can create distributed applications using these tools. However, each one presents unique challenges,

often requiring advanced programming techniques and development of custom data handling mechanisms. It provides users to LabVIEW remote panels. One of the first things in LabVIEW application development is that VIs consists of front panels, diagrams, and behind the scenes, compiled executable code. Furthermore, these components are always bound together for a VI that is executing. The front panel and compiled code have both been required for operating a front panel.

The SMA experiment is implemented and run by programed VI of LabVIEW in the workstation. The VI has several parts as we have mentioned in previous chapters, such as sliding mode control codes, and PWM codes. In this section, we will discuss more about the implementations of sliding mode based controller and PWM in LabVIEW.

Implementation of sliding mode-based controller in LabVIEW

The displacement control in the SMA experiment is using a sliding mode based controller. As shown in [Figure 8](#), the control has two parts, measurement of the displacement and computation of the real-time control. The measurement of the displacement is performed by an electrically powered linear sensor. The sensor generates voltage output as response to the displacement of the SMA wire in a mathematically linear relation. The conversion from the voltage measurement to the displacement measurement is implemented using LabVIEW. In the [Figure 9](#), we have the LabVIEW code of showing how the conversion from the measured displacement in voltage to the displacement in inch is implemented in the real experiment. The relation can also be expressed in the following equation,

$$D(\text{in}) = \frac{D(\text{volts}) - 2.048}{4.63 \times 0.039318} \quad (11)$$

Where 2.048 is a tuned constant for the real experiment, 4.63 is the driving voltage of the linear sensor, and 0.039318 is a constant predetermined by the manufacturer of the linear sensor used for the conversion from voltage measurement to displacement measurement.

The sliding mode based controller expressed in [Equation \(1\), \(2\), and \(14\)](#) are implemented in LabVIEW as shown in [Figure 10](#). The parameters of the sliding mode based controller are tuned in the experiment. New form of the equation is expressed in the following,

$$V = V_f - Kr - \rho \tanh(ar). \quad (12)$$

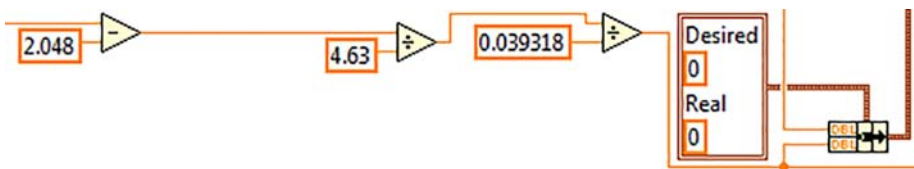


Figure 8: Displacement measurement code in LabVIEW.

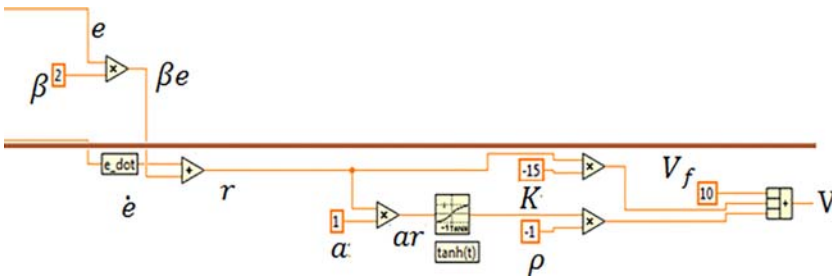


Figure 9: Implementation of sliding mode based controller in LabVIEW.

After tuning in the experiment, Eqn. (2) and Eqn. (13) become,

$$r = \dot{e} + 15e \tag{13}$$

$$V = 10 - 15r - 1 \tanh(-1r), \tag{14}$$

Where V is the output voltage.

In LabVIEW, the error in Equation (1) can be calculated by letting the desired value of displacement subtract the value of the measured displacement. The control variable of r is expressed in the terms of the variable of error and the variable of the derivative of error. The derivative of error is calculated by dividing the error of displacement by the time difference between each data measurement. The function of tanh is provided in LabVIEW and we can use it directly. The feedforward constant V_f is tuned to be 10 volts to compensate for the heat loss in the environment. Other constants of the controller are tuned based on the performance of the SMA experiment. It has a disadvantage that if any big environmental change or external change occurred to the SMA experiment, the parameters in the controller would need slight modifications.

Implementation of pulse width modulation in LabVIEW

In the implementation of PWM, we have two signals, carrier signal and reference signal, to be compared. We use an express VI from LabVIEW to simulate a triangle signal as our reference signal. The configuration of the reference signal for the SMA experiment is 12.5Hz in frequency, 3.5 in amplitude, and 8 for offset. There are 50 samples per second and five samples are

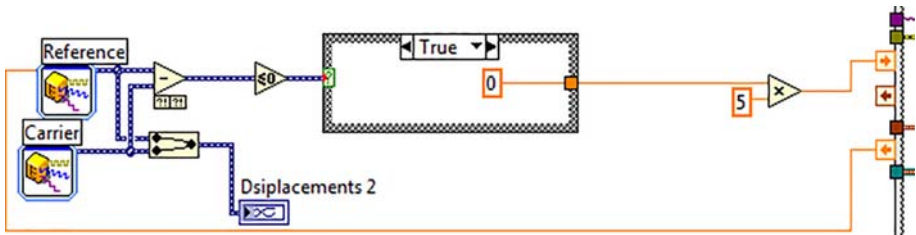


Figure 10: Implementation of PWM in LabVIEW.

generated per loop. In other words, every triangle in the reference signal needs 100ms to be generated. The carrier signal is generated by using the same express VI as used for the reference signal with the signal type to be DC rather than triangle. The configuration of the DC signal is eight for offset, and the simulate acquisition rate is 50 samples per second and 5 samples per loop, which is the same as the simulate acquisition rate for the triangle signal. The same simulate acquisition rate between the reference signal and the carrier signal makes two signals comparable in calculation. In the comparison of two signals, once the amplitude of the carrier signal is larger than the amplitude of the reference signal, the value of pulse is positive. In the implementation of such a comparison in LabVIEW, we subtract the reference signal from the carrier signal and compare the value after subtraction to zero. If the value is negative or less than zero, the Boolean VI of less and equal to zero returns true to the case structure, otherwise, it returns false to the case structure. The return from the case structure is zero when it is true and one when it is false. The value is amplified by five and returns to the VI of data output. Repeating of the algorithm will create the PWM signal.

The SMA Experiment based on LabVIEW has its own remote panel, as shown in Figure 11. It can be easily created in the VI application. Once the programming in LabVIEW is done, users can use the Web Publishing Tool to create a website for remote control. In order to run the remote panel to control the real VI application, users need to install LabVIEW run-time engine in their computer. Figure 11 depicts a LabVIEW remote panel used in traditional version of remote lab. This remote panel is displayed in a web browser and the users can use it as they are using LabVIEW. In this remote lab, users are able to perform voltage control, position control and

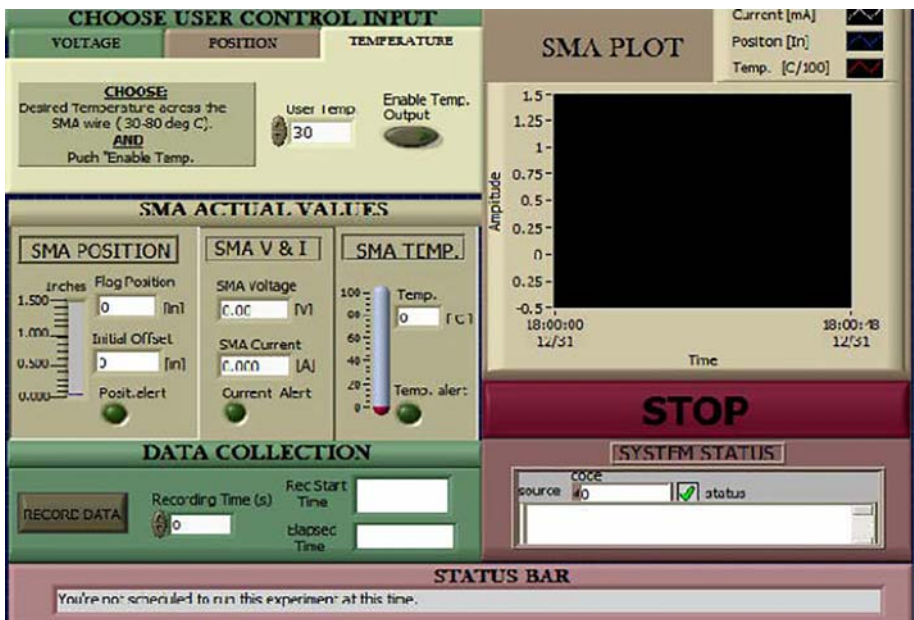


Figure 11: SMA experiment LABVIEW Remote Panel.

temperature control through the web remotely on the real experiment. The data, in terms of temperature, voltage and displacement, are displayed in this panel too.

Table 1 compares the differences between LabVIEW remote panel in web browsers and remote panel in the LabVIEW environment. With the LabVIEW, remote front panels not only can be viewed, but can also be controlled from either the LabVIEW environment or a web browser. This powerful tool will enable many programmers to create distributed applications easily.

LabVIEW, users also can operate the front panel on a machine that is separate from where the VI resides and executes. Furthermore, they can embed the front panel into a web page and operate it within that page. All that is required on the client machine for executing in a web page is a browser and the LabVIEW runtime engine and browser plug-in. As requiring administrator privileges, the LabVIEW's runtime engine cannot be installed on any public computer by normal users. Students cannot use their own computer to install the LabVIEW's runtime engine at home, and therefore it limits the time availability to the students learning.

In order to resolve the LabVIEW's runtime engine and software plug-in installation issues, we designed and implemented a novel unified framework for new remote laboratory development. As the good example, the new remote SMA experiment was developed. The goal of this work is to provide users a remote experiment interface that will work with any web browser.

Remote SMA experiment based on a novel unified framework

The novel unified framework includes three parts, client web application, server application and experiment control application. The client web application is based on HyperText Markup Language (HTML), Cascading Style Sheets (CSS), and JQuery/JQuery-Mobile JavaScript libraries. Mashup technology is used for user interface implementation.

The client web application can be run in most of current popular browsers such as IE, Firefox, Chrome, Safari etc. The server application is based on Web Service technology, and is directly built on top of MySQL database, Apache web server engine and Node.js web server engine

Table 1: Compilation list between Remote Panels in a Web Browser and LabVIEW.

	Web Browsers	LabVIEW
1	Only the LabVIEW run-time Engine and browser plug-in are required on the client machine. The LabVIEW development environment is not requirement	The LabVIEW environment (or a LabVIEW executable with a menu option to run remote panels) and LabVIEW run-time are required. A web browser is not required.
2	The browser allows connecting to the local program on the same machine as the server. (http://localhost/name of (the VI.html))	Connecting to the remote panel from LabVIEW on the same machine as the server is not permitted.
3	Only the "operate" menu is available in browser's remote panel.	Regular LabVIEW menu options are available with certain items disabled.
4	An HTML file must be created to control remote panel in the web browser. Once the HTML page is created, any changes to the front panel are automatically reflected in the remote panel viewed in the web browser.	An HTML page is not required.

Table 2: Technology/protocol/software list for the new framework.

	Name	Technology/Protocol/Software	Remark
1	Http Proxy	Node-HTTP-Proxy	Part of Node.js
2	Data Protocol	Socket.IO	Part of Node.js
3	Real-time experiment video Transmission	Http Live Streaming Protocol/FFMPEG/ Segmenter software package	
4	Database	MySQL	
5	Client – User Interface	Mashup technology, JavaScript	
6	Server - Web Service	Apache (2.2), Node.js (V1.0), JSON	LtoN (LabVIEW to Node.js)
7	Equipment Control	LabView (V. 2012)	

(Hughes-Croucher and Wilson 2012, Herron 2013). The server application uses JSON and Socket.IO which is developed based on web socket protocol to implement the real-time communication between the server application and the client-web application (Rai 2013). The server application runs on Centos 6.0 Linux server.

The experiment control application is based on the LabVIEW, and uses Socket.IO for real time communication with server application. The experiment control application runs on experiment control workstation which runs Window 7 OS. Our new unified framework for remote laboratory development is based on three vital technologies, which are the Socket.IO, Node-HTTP-Proxy, and HLS protocol. Node-HTTP-Proxy is used for experiment data and control commands transmission and traversing firewall and the novel video transmission approach is based on HLS protocol for real-time system monitoring. Mashup technology is used for user interface implementation.

Table 2 depicts the technical characteristics of the new unified framework in detail.

The implementation of the new remote SMA experiment

In order to implement the new remote SMA experiment, three things need to be completed; the user interface development, system integration on the server side, and integrating the LtoN module to the new SMA experiment.

The user interface development

In the implementation of the client web application, we use the Web 2.0 technology which includes HyperText Markup Language (HTML), Cascading Style Sheets (CSS), and JQuery/JQuery-Mobile JavaScript libraries. Table 3 depicts the technology, protocol and software used in the client web application development.

Table 3: Technology/protocol/software list for the Client web application.

	Name	Technology/Protocol/Software	Remark
1	Development Language	HTML, CSS, JavaScript	Using HTML5
2	Real-Time communication Protocol	Socket.IO	Part of Node.js
3	Integration technology	Mashup technology	
4	Widgets	JQuery/ JQuery-Mobile	



Figure 12: Sample Paradigms of the New SMA Experiment user interface.

In addition, the Mashup technology for user interface integration is employed in our client application. We use server-based Mashup technology to generate our client application. Server-based Mashup analyzes and reformats the data on a remote server and transmits the data to the user's browser. Figure 12 depicts three sample paradigms of the client application which shows three different user interfaces for new remote SMA experiment. The architecture of our Mashup scheme is divided into three layers:

- Presentation / user interaction: this is the user interface of Mashup. Our novel design uses HTML, CSS, JavaScript and Asynchronous JavaScript.
- Web Services: the system functionality can be accessed using the API services. Our novel design used JSON-RPC, REST and SOAP.
- Data: the data is handled in three ways, i.e., sending, storing and receiving. Our novel design uses JSON and Socket.IO for data transmission.

Server-side integration

The server application is directly built on the top of a novel assembled server engine scheme, and it includes two server engines working together, Apache HTTP server engine and Node.js server engine. Based on the server-based Mashup technology used in the novel framework, the Apache HTTP server application integrates the user interface widgets with web content and the real-time experiment video, and Node.js server application handles the real time experiment data transmission. Table 4 depicts the technology, protocol and software used in the server application implementation.

Table 4: Technology/protocol/software list for the Server application.

	Name	Technology/Protocol/Software	Remark
1	Server Engine	Apache 2.4.6, Node.js 0.10.21	Using the newest stable version
2	Real-Time experiment data Protocol	Socket.IO	Part of Node.js
3	Database	MySQL 5.5	
4	HTTP Proxy	Node-HTTP-Proxy	Part of Node.js
5	Real-Time video transmission	Http Live Streaming Protocol/FFMPEG/Segmenter software package	

We implemented the experiment scheduler system and user management system on the server-side. For the data management, we use the MySQL 5.5 Database management system.

Integrate LtoN module to the new SMA experiment

We designed and developed a new real time experiment data transmission protocol based on Socket.IO and JSON. It is named LtoN (LabVIEW to Node.js). Using the new real time transmission protocol, an end user can conduct the experiment, save the experiment data, and load the experiment data file. More details of this new protocol are introduced in the following:

- The new application communication protocol includes two parts, client part running in browsers and server part running in web server. They are developed by JavaScript language and enhanced by the web socket protocol.
- In this new application transmission protocol, we defined our own special communication instruction set to implement real time experiment control commands and experiment data transmission. With the new communication instruction set, we can secure the data communication when user is conducting the remote experiment.
- In our new protocol, we designed some brief instruction to control experiment progress to improve the experiment data transmission performance.

For the protocol implementation, we only need to create two JavaScript files, one for client application running in web browsers and the other one for the server application running in web server. Then we need to create the new Node.js task to run the protocol in server-side, and this server-side application must hold running status forever. Because only the server-side protocol application holds the status active, it can ensure the normal real time communication. On the client side, there is a set file of communication instruction functions to support the normal operation of the client application in web browsers.

Table 5: Technology/protocol/software comparison list between two solutions.

	Function Name	New Remote SMA Experiment with the Novel Unified Framework	Remote SMA Experiment with LabVIEW
1	Traversing network firewall	Node-HTTP-Proxy	None
2	Data Protocol	LtoN (LabVIEW to Node.js) data transaction protocol	NI Publish-Subscribe Protocol (NI-PSP)
3	Real-time experiment video	HTTP Live Streaming Protocol/ FFMPEG/Segmenter software package	None
4	Database	MySQL	MySQL
5	Client - User Interface	Mashup technology, JavaScript	LabVIEW Remote Panel
6	Software Plug-in	None	LabVIEW run-time engine and browser plug-in
7	Server - Web Service	Apache (2.2), Node.js (V1.0), JSON	LabVIEW Web Service
8	Equipment Control	LabVIEW (V. 2012)	LabVIEW (V. 2012)

Table 6: The advantages of the new remote SMA experiment.

	Advantage Function Name	New Remote SMA Experiment with the Novel Unified Framework	Remote SMA Experiment with LabVIEW
1	Traversing network firewall	Node-HTTP-Proxy	None
2	Real-time experiment video	Http Live Streaming Protocol/FFMPEG/Segmenter software package	None
3	Software Plug-in	None	LabVIEW run-time engine and browser plug-in

Comparison of two remote SMA experiments

Table 5 lists the development technologies, experiment data transaction protocols and software packages which are used in these two solutions. It is clear that the new solution makes some improvements in traversing network firewall function and is software plug-in free. In order to provide a more realistic experience to the user for conducting the remote SMA experiment, the new solution also implements the Real-Time experiment video function.

Comparing to the traditional remote SMA experiment with the LabVIEW remote panel, as Table 6 depicts, the new SMA remote experiment solution has three advantages. The user interface of the new remote SMA experiment is plug-in free and running in different web browsers, and the new solution also resolves the traversing network firewall issue. End users only need to access the Internet and use a web browser to operate the SMA experiment. The experiment control webpage is developed by JavaScript, which is a universal and regular computer language. Meanwhile, any regular web browsers are good to use all the features

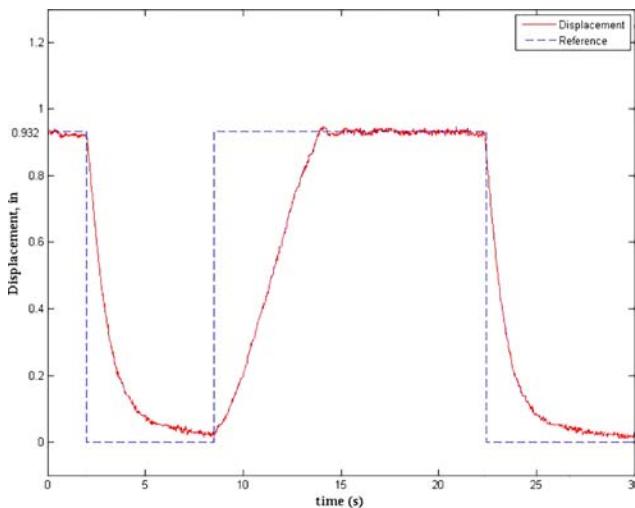


Figure 13: Arbitrary displacement control (with amplitude of 0.932in) in remote SMA experiment.

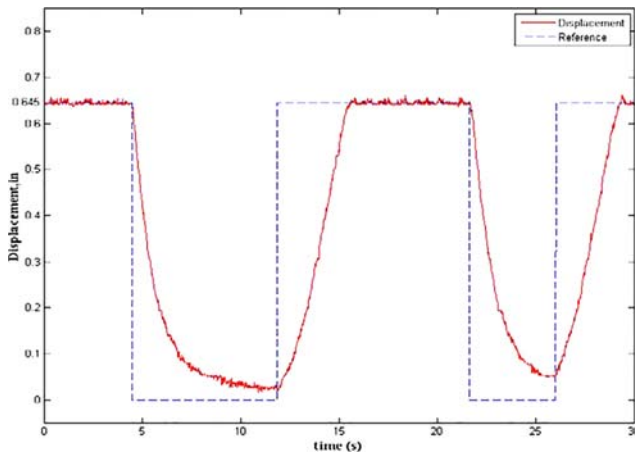


Figure 14: Arbitrary displacement control (with amplitude of 0.646in) in remote SMA experiment.

of the remote panel without requiring any more extra software plug-ins. In addition, the new remote SMA experiment provide the real-time experiment video function, it provides a more realistic experience to the user for conducting the remote SMA experiment. This new remote SMA experiment user interface can also be used through smart phones and tablet computer.

The experiment data collected from the new remote SMA experiment with the novel unified framework shows no big difference to the data recorded using remote SMA experiment with LabVIEW, except for the amplitude of the reference. The amplitude can be different because they are defined by the users. The data recorded from the new remote SMA experiment GUI has fewer samples per second comparing to that in remote SMA experiment with LabVIEW.

The data transmission in the GUI is limited to 140 samples per second to minimize the memory and increase the connection speed. In remote SMA experiment with LabVIEW, the sampling rate is 1000 samples per second; however, by comparing from [Figure 13](#) and [Figure 14](#) with the experimental results, the hysteresis of SMA has been successfully demonstrated by the data recorded in the new remote SMA experiment with the novel unified framework which matches the original results collected locally.

Conclusion

In this paper, we have illustrated and compared the two different implementation approaches for a remote SMA experiment. A new remote SMA experiment was successfully implemented under this new unified framework and the user interface can be run on any web browsers in any platform without installing any additional software plug-in. The capability of running remote experiment on portable device let users gain insights by observing and interacting with the real instrument in an efficient way.

Acknowledgements

This material is based upon work supported by the Qatar National Research Fund under Grant No. NPRP 4-892-2-335.

Sponsor acknowledgement

Maersk Oil Qatar is the exclusive sponsor and industry partner for Engineering Education Letters, an open access, peer-reviewed journal that promotes the advancement of engineering education in the Middle East, North Africa and beyond. Publication costs for this manuscript are supported by Maersk Oil Qatar, which has no influence on journal content or editorial decisions. For further details, see the Engineering Education Letters Transparency Statement.

References

- Black, H. S. (1953). *Modulation Theory*, Van Nostrand Reinhold, New York.
- Bowes, S. R., & Grewal, S. (1998). Modulation strategy for single phase PWM inverters. *Electron. Lett.*, 34(5), 420–422.
- Boost, M. A., & Ziogas, P. D. (1988). State-of-the-art carrier PWM techniques: A critical evaluation. *IEEE Trans. Ind. Appl.*, 24(2), 271–280.
- Bang, H., Ha, C., & Kim, J. H. (2005). Flexible Spacecraft Attitude Maneuver by Application of Sliding Mode Control. *Acta Astronautica*, 57(11), 841–850.
- Cai, L., & Abdalla, A. (1993). A smooth tracking controllers for uncertain robot manipulator. *Proc. IEEE Int. Conf. on Robotics Autom.*, (pp. 83–88), Atlanta, GA.
- Cai, L., & Song, G. (1993). A smooth robust nonlinear controller for robot manipulator with joint stick-slip friction. *Proc. IEEE Int. Conf. on Robotics Autom.*, (pp. 449–454), Atlanta, GA.
- Cepeda-Gomez, R., Olgac, N., & Sierra, D. A. (2010). Application of Sliding Mode Control to Swarms under Conflict. *IET Control Theory and Applications*, 5(10), 1167–1175.
- Duro, N., Dormido, R., Vargas, H., Dormido-Canto, S., Sanchez, J., Farias, G., ... Esquembre, F. (2008). An Integrated Virtual and Remote Control Lab: The Three-Tank System as a Case Study. *Computing in Science & Engineering*, 10(4), 50–59.
- Fan, B., & Song, G. (2005). Hysteresis in a Shape Memory Alloy Wire: Identification and Simulation. Conference Proceeding Smart Structures and Materials 2005: Modeling, Signal Processing, and Control.
- Gillet, D., Salzmann, C., Longchamp, R., & Bonvin, D. (1997). Telepresence: An Opportunity to Develop Real-World Experimentation in Education. European Control Conference, Brussels, Belgium, Session WE-M-L 1(July 1-4, 1997).
- Grant, D., & Hayward, V. (1997). Variable structure control of shape memory alloy actuator. *IEEE Control syst. Mag.*, 17, 80–88.
- Gravier, C., Fayolle, J., Bayard, B., Ates, M., & Lardon, J. (2008). State of the Art About Remote Laboratories Paradigms—Foundations of Ongoing Mutations DIOM Laboratory. *ijOE*, 4(1), 18–25.
- Hughes-Croucher, T., & Wilson, M. (2012). Up and Running with Node.js (First ed.). *O'Reilly Media*, p. 204, ISBN 978-1-4493-9858-3.
- Herron, D. (2013). *Node Web Development*. Second Edition, Packt Publishing. ISBN 184951514X.
-

- Kilicarslan, A., Song, G., & Grigoriadis, K. (2008). ANFIS Based Modeling and Inverse Control of a Thin SMA Wire. *Proceeding of Modeling, Signal Processing, and Control for Smart Structures*, 6926(1).
- Kizmaz, H., Aksoy, S., & Muhurcu, A. (2010). Sliding Mode Control of Suspended Pendulum. *Modern Electric Power Systems*, 1–6.
- Lentijo, S., Pytel, S., Monti, A., Hudgins, J., Santi, E., & Simin, G. (2004). FPGA Based Sliding Mode Control for High Frequency Power Converters. *IEEE 35th Annual Power Electronics Specialists Conference*, 5, 3588–3592.
- Lowe, G. K., & Zohdy, M. A. (2010). Modeling Nonlinear Systems Using Multiple Piecewise Linear Equations. *Nonlinear Analysis: Modeling and Control*, 15(4), 451–458.
- Majima, S., Kodama, K., & Hasegawa, T. (1999). Modeling of shape memory alloy actuator and tracking control system with the model. *IEEE Trans. Control Syst. Technol.*, 7, 511–528.
- Rai, R. (2013). Socket. IO Real-time Web Application Development. *O'Reilly Media*, ISBN 178-2-1607-87.
- Song, G., & Mukherjee, R. (1998). A Comparative Study of Conventional Non-Smooth Time-Invariant and Smooth Robust Compensator. *Transaction on IEEE, Control Systems Technology*, 6(4).
- Song, G., & Quinn, D. (2004). Experimental Study of Robust Tracking Control a Shape Memory Alloy Wire Actuator. *Journal of Dynamic Systems, Measurement, and Control*, 126(3), 674.
- Song, G., & Ma, N. (2007). Robust Control of a Shape Memory Alloy Wire Actuated Flap. *Smart Mater. Struct.*, (6), N51–N57.
- Sehab, R. (2007). Fuzzy PID Supervision for a Nonlinear System: Design and Implementation. 2007 Annual Meeting of the North American Fuzzy Information Processing Society, (pp. 36–41).
- Tai, N. T., & Ahn, K. K. (2010). A RBF Neural Network Sliding Mode Controller for SMA Actuator. *International Journal of Control, Automation, and Systems*, 8(6), 1296–1302.
- Vasca, F., & Lannelli, L. (2012). Dynamics and Control of Switched Electronic Systems Advanced Perspectives for Modeling. *Simulation and Control of Power Converters*, 492.
- Wang, N., Chen, X., Song, G., & Parsaei, H. (2014). Remote Experiment Development Using an Improved Unified Framework. *Proceedings of World Conference on E-Learning in Corporate, Government, Healthcare, and Higher Education 2014 (2003–2010)*, AACE, Chesapeake, VA.
-